Data S2: Structural determination of selected MDM metabolites

Contents:

A. Capecitabine and deglycocapecitabine

The expected molecular formula of deglycocapecitabine ($C_{10}H_{14}FN_3O_3$) was deduced from HR-MS data (**Table S1**). To confirm its structure, we isolated pure deglycocapecitabine using HPLC. ^{1}H-NMR spectrum of deglycocapecitabine was almost identical to that of capecitabine, except for the absence of the sugar moiety (**Table 1 and Figure 1**) and the presence of one proton of 1-NH at chemical shift 11.16 ppm. MS/MS experiments confirmed the absence of the sugar in deglycocapecitabine as compared to capecitabine (**Figure 2**). Altogether, the results confirmed the structure of the metabolite as deglycocapecitabine.

Table 1. ^{1}H NMR data for capecitabine and purified deglycocapecitabine (500 MHz in DMSO-D6)

Position	δH, mult (*J* in Hz) Capecitabine	δH, mult (*J* in Hz) Deglycocapecitabine
1-NH	ND*	11.16, br
2		
3		
4		
5		
6-CH	8.01, s	7.95, s
7-NH	10.52, br	11.16, br
8		
9-CH$_2$	4.07, m[b]	4.05, t
10-CH$_2$	1.61, p	1.60, p
11-CH$_2$	1.32, m[b]	1.32, m[b]
12-CH$_2$	1.32, m[b]	1.32, m[b]
13-CH$_3$	0.88, t	0.88, m[b]
14-CH	5.67, d	ND
15-CH **-OH**	4.09, m[b] 5.14	ND
16-CH **-OH**	3.68, t 5.14, br	ND
17-CH	3.90, p	ND
18-CH$_3$	1.31, m[b]	ND

[b] overlapped signal
*ND: Not Detected

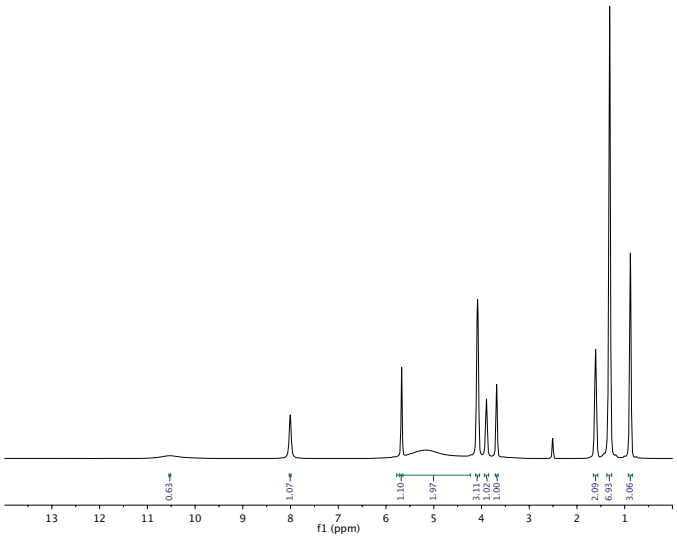

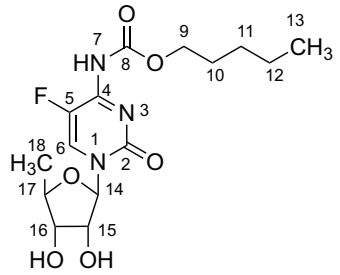

capecitabine

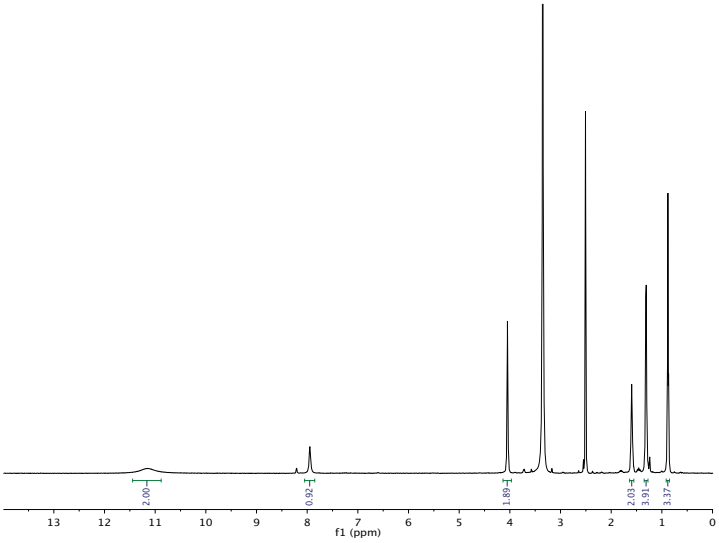

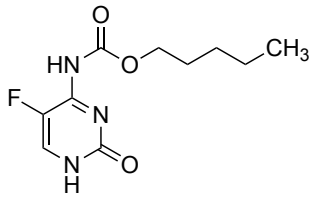

deglycocapecitabine

Figure 1. ^{1}H NMR spectra of capecitabine and purified deglycocapecitabine in DMSO-D6

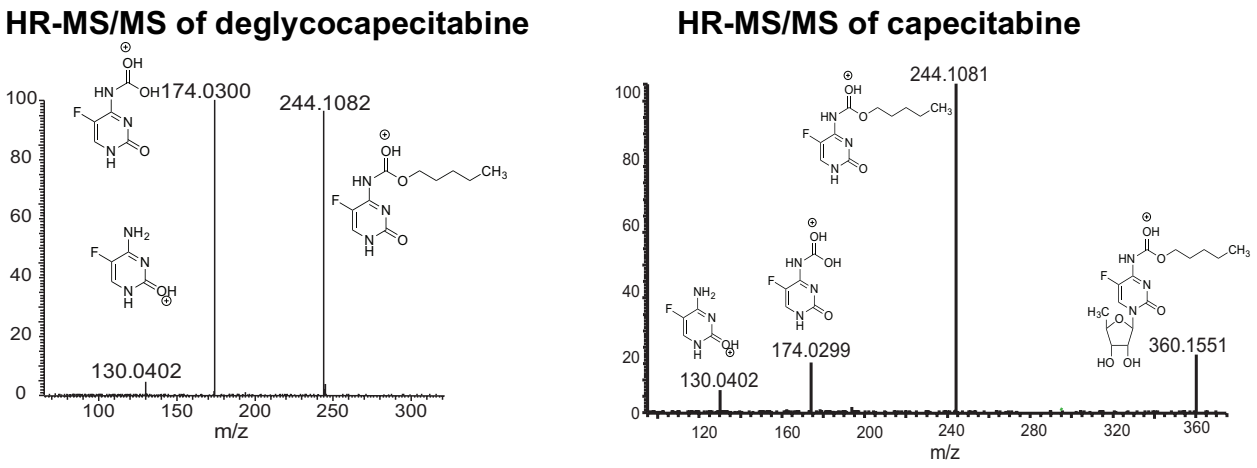

Figure 2. HR-MS/MS analysis of capecitabine and deglycocapecitabine (protonation position is arbitrary).

B. Hydrocortisone and 20β-dihydrocortisone

The molecular formula of dihydrocortisone ($C_{21}H_{32}O_5$) was deduced from HR-MS data (**Table S1**), implying a reduction to the parent molecule. To elucidate the structure of the metabolite and localize the position of this modification, we isolated pure dihydrocortisone using HPLC. ^{13}C -NMR, ^{1}H-NMR, and 2D-HSQC NMR spectra of dihydrocortisone were almost identical to those of hydrocortisone, except for: 1) The shift of the ketone carbon C-20 from chemical shift 211.7 ppm to 75.2 ppm, and the relocation of the methylene protons at C-21 from 4.08 and 4.51 ppm to 3.40 and 3.46 ppm, which resulted from the shielding effect of the hydroxyl group at C-20; and 2) The presence of a methine proton at C-20 at chemical shift 3.56 ppm (**Table 2 and Figures 3-5**). Altogether, the results confirmed the structure of the metabolite as 20-dihydrocortisone, which is derived from the ketone reduction of hydrocortisone. To determine the stereochemistry of the hydroxyl group at C-20, we compared our dihydrocortisone metabolite to authentic standards of 20α-dihydrocortisone and 20β-dihydrocortisone using HPLC-HRMS following the same column, gradient, and analysis methods as for the donor runs. Our MDM metabolite had the same retention time as 20β-dihydrocortisone (**Figure 6**).

Table 2. ^{1}H NMR data for hydrocortisone and purified 20β-dihydrocortisone (500 MHz in DMSO-D6)

Position	δH, mult (*J* in Hz) Hydrocortisone	δC	Position	δH, mult (*J* in Hz) 20-dihydrocortisone	δC
1-CH_2	2.43, m[b]	31.4	**1-CH_2**	1.32, 1.70	33.2
2-CH_2	2.57, t	33.0	**2-CH_2**	2.43, 2.19	31.5
3		198.1	**3**		198.1
4-CH	5.56, s	121.5	**4-CH**	5.55,s	121.4
5		172.4	**5**		172.8
6-CH_2	2.41, 2.20, m[b]	33.5	**6-CH_2**	2.18, 2.36	33.5
7-CH_2	1.65,1.27, m[b]	23.4	**7-CH_2**		23.8
8-CH	1.65, dd	51.6	**8-CH**	1.5	50.3
9-CH	1.91, m[b]	31.2	**9-CH**	1.87	31.3
10		38.9	**10**		38.9
11-CH	4.26, m	66.5	**11-CH**	4.22, m	66.7
12-CH_2	1.88, 1.54, m[b]	39.1	**12-CH_2**	1.90, 1.63	40.9
13		46.4	**13**		46.5
14-CH	0.86, m	55.6	**14-CH**	0.83, m	55.8
15-CH_2	1.93, 0.99, m[b]	32.8	**15-CH_2**	1.92, 0.95	33.0
16-CH_2	2.09,1.79, m[b]	34.1	**16-CH_2**	2.10, 1.77	34.1
17		88.5	**17**		84.1
18-CH_3	0.75, s	17.0	**18-CH_3**	0.98	17.1
19-CH_3	1.37, s	20.5	**19-CH_3**	1.38	20.5
20		211.7	**20-CH**	3.56, m[b]	75.2
21-CH_2	4.51, 4.08, dd	65.9	**21-CH_2**	3.45, 3.40, m[b]	63.8

[b] overlapped signal
*ND: Not Detected

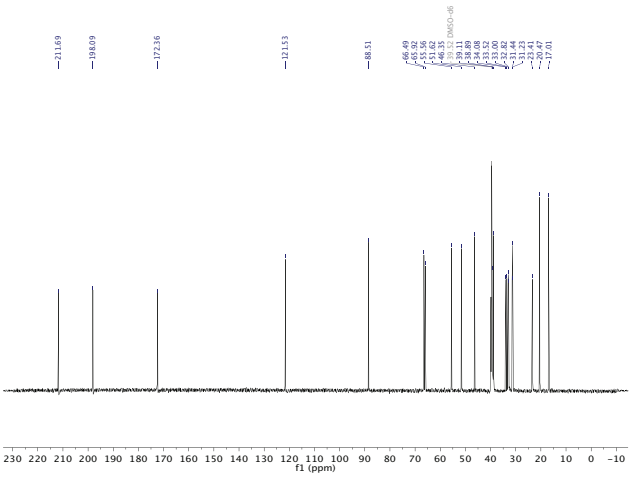

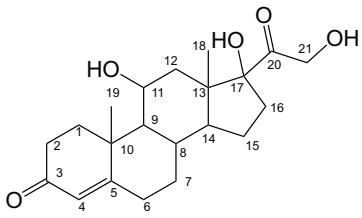

hydrocortisone

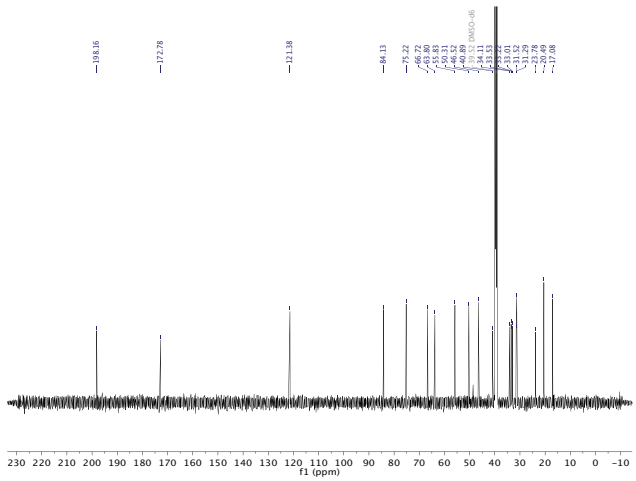

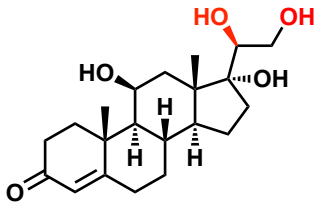

20β -dihydrocortisone

Figure 3. ^{13}C NMR spectra of hydrocortisone and purified 20β-dihydrocortisone in DMSO-D6

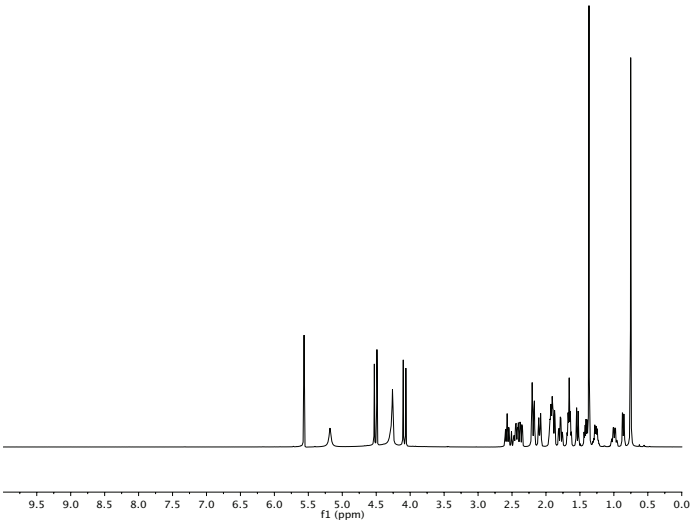

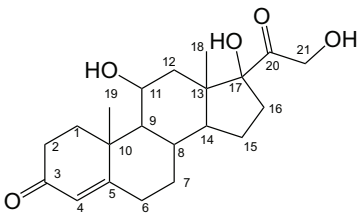

hydrocortisone

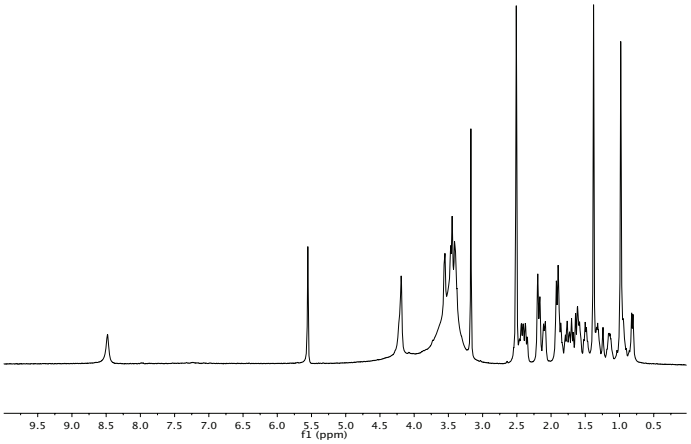

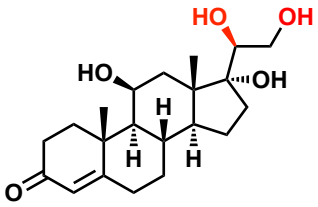

20β-dihydrocortisone

Figure 4. ^{1}H NMR spectra of hydrocortisone and purified 20β-dihydrocortisone in DMSO-D6

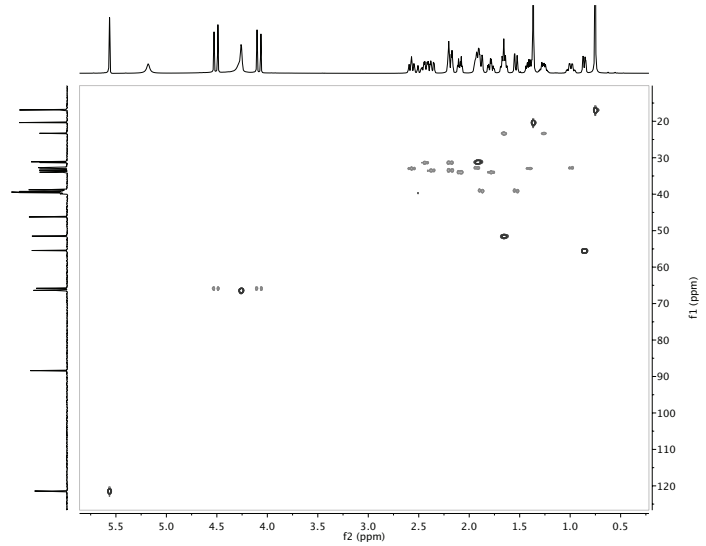

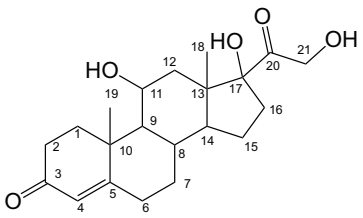

hydrocortisone

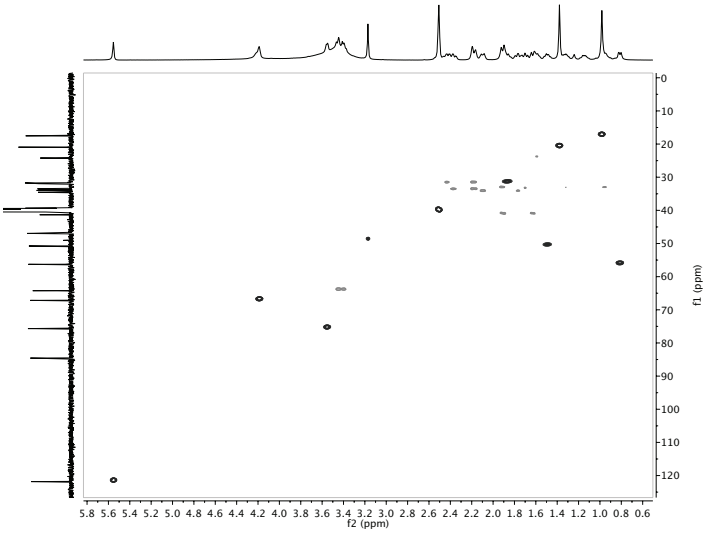

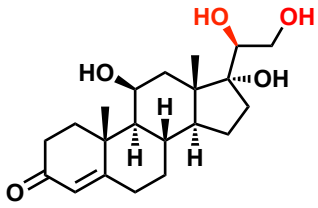

20β-dihydrocortisone

Figure 5. HSQC spectra of hydrocortisone and purified 20β-dihydrocortisone in DMSO-D6

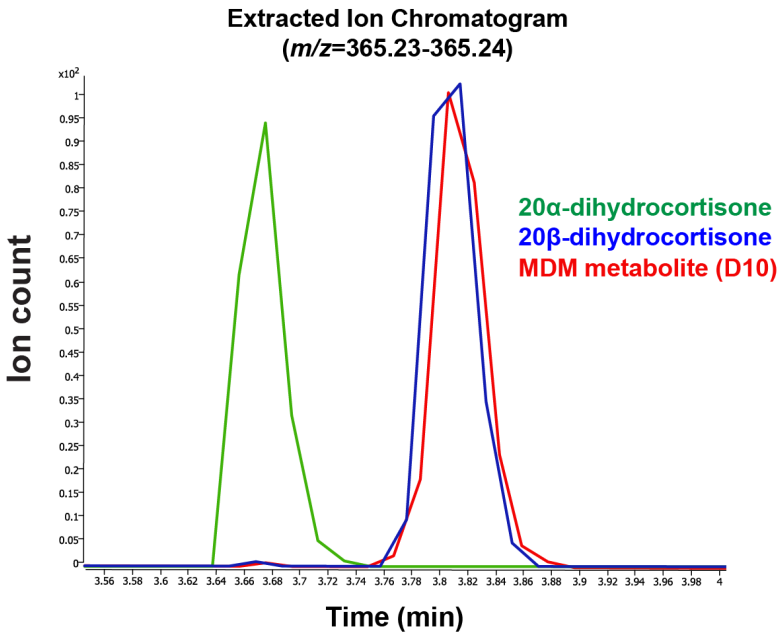

Figure 6. HPLC-HRMS analysis of the MDM metabolite of hydrocortisone in comparison to authentic standards of 20α-dihydrocortisone and 20β-dihydrocortisone.

C. Tolcapone and *N*-acetylamino-tolcapone

The tolcapone metabolite was purified and its structure was elucidated using 1D and 2D NMR analyses.

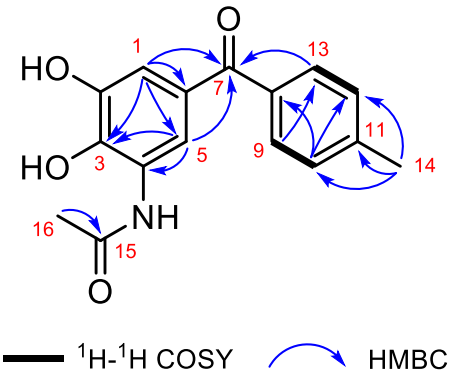

Figure 7. ^{1}H-^{1}H COSY, key HMBC correlations of purified *N*-acetylamino-tolcapone.

Table 3. ^{1}H and ^{13}C NMR data (δ in ppm, J in Hz) for *N*-acetylamino-tolcapone in MeOD.

No.	***N*-acetylamino-tolcapone** [a]	
	δ_H (mult)	δ_C type
1	7.66 brs	119.0 CH
2	–	–[b] qC
3	–	143.3 qC
4	–	147.1 qC
5	7.18 s	114.2 CH
6	–	126.8 qC
7	–	197.5 qC
8	–	136.7 qC
9	7.67 brs	131.0 CH
10	7.35 s	129.9 CH
11	–	144.2 qC
12	7.35 s	129.9 CH
13	7.67 brs	131.0 CH
14	2.45 s	21.6 CH_3
15	–	172.6 qC
16	2.20 s	23.4 CH_3

[a] Recorded at 500 MHz and 125 MHz for ^{1}H and ^{13}C NMR, respectively, in MeOD, chemical shifts (ppm) referred to MeOH (δ_H 3.31, δ_C 49.0). [b] not detected. Assignments were deduced by analysis of 1D and 2D NMR spectra.

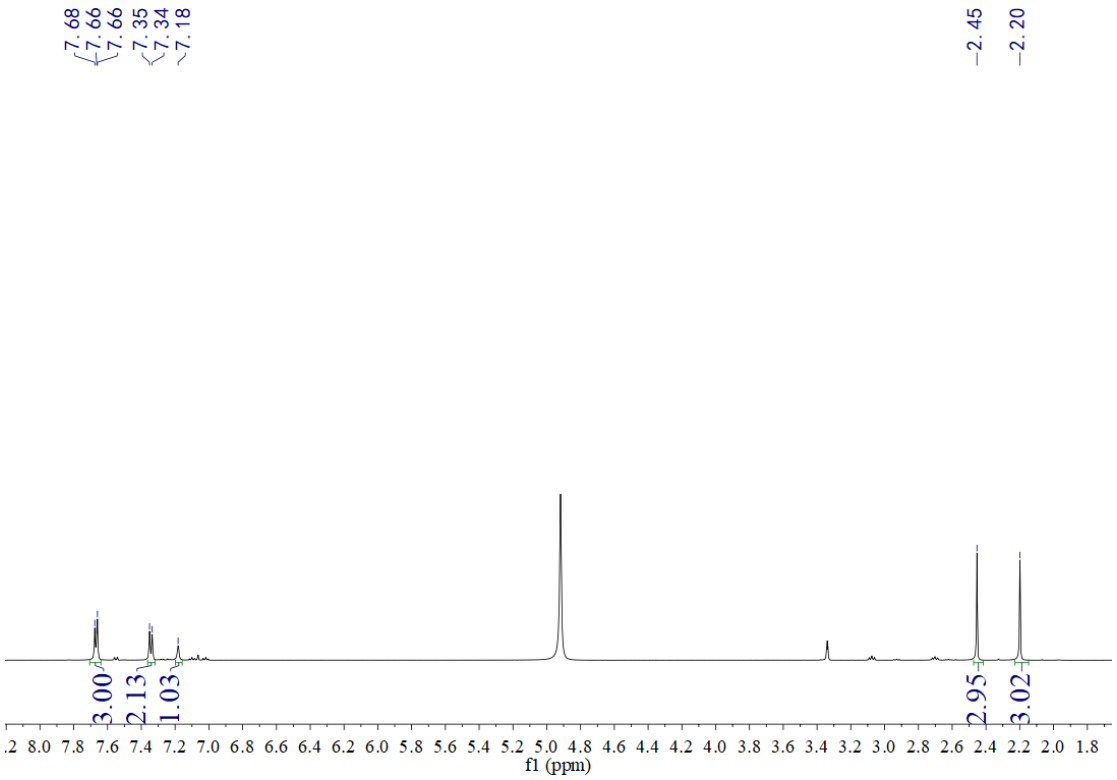

Figure 8. [1]H NMR spectrum (500 MHz) of purified *N*-acetylamino-tolcapone in MeOD.

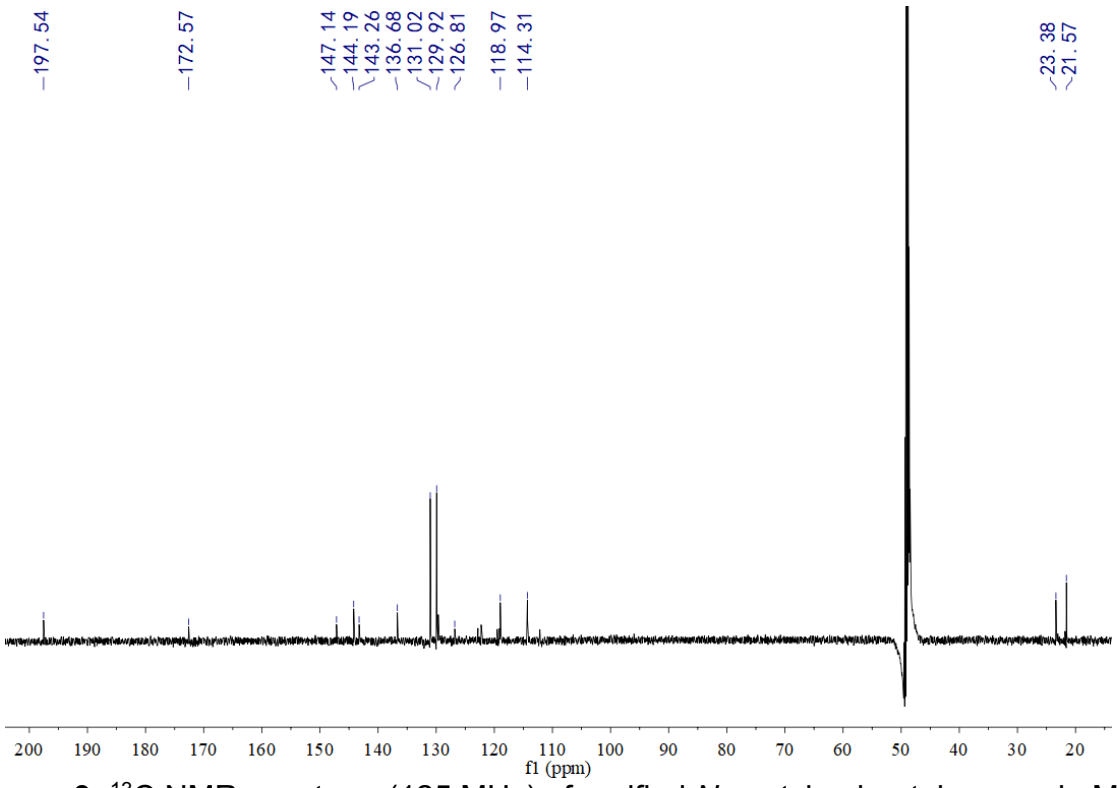

Figure 9. [13]C NMR spectrum (125 MHz) of purified *N*-acetylamino-tolcapone in MeOD.

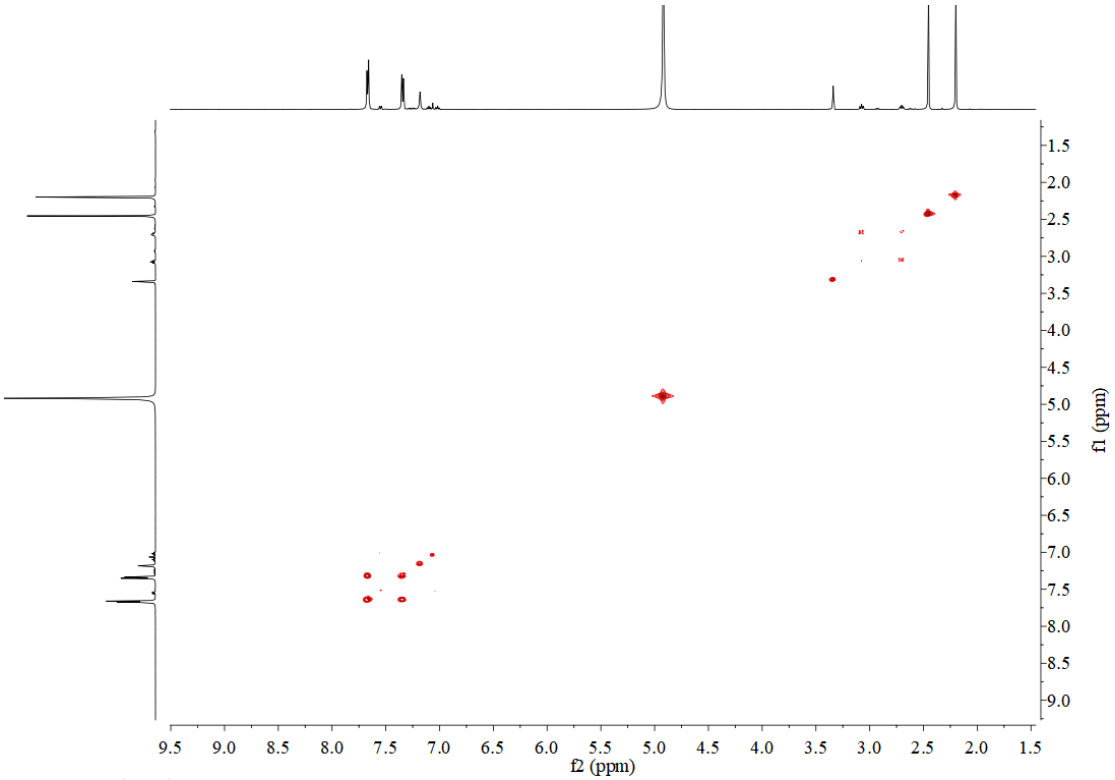

Figure 10. ^{1}H-^{1}H COSY spectrum (500 MHz) of purified *N*-acetylamino-tolcapone in MeOD.

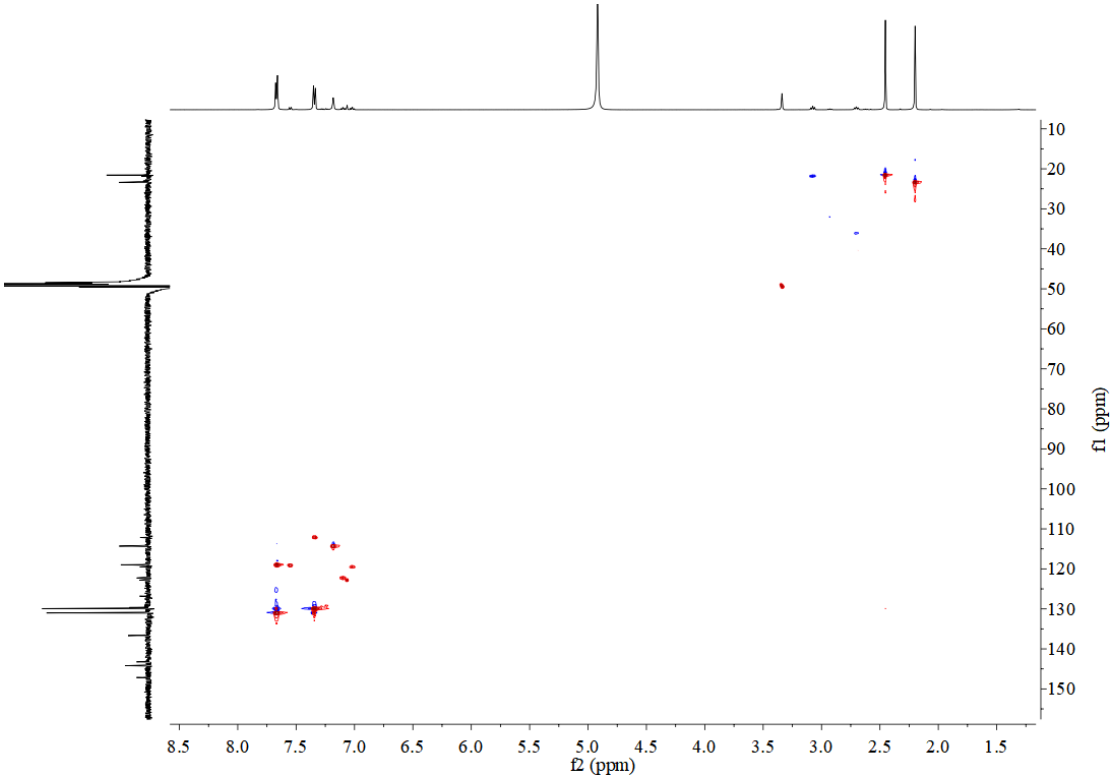

Figure 11. HSQC spectrum (500 MHz) of purified *N*-acetylamino-tolcapone in MeOD.

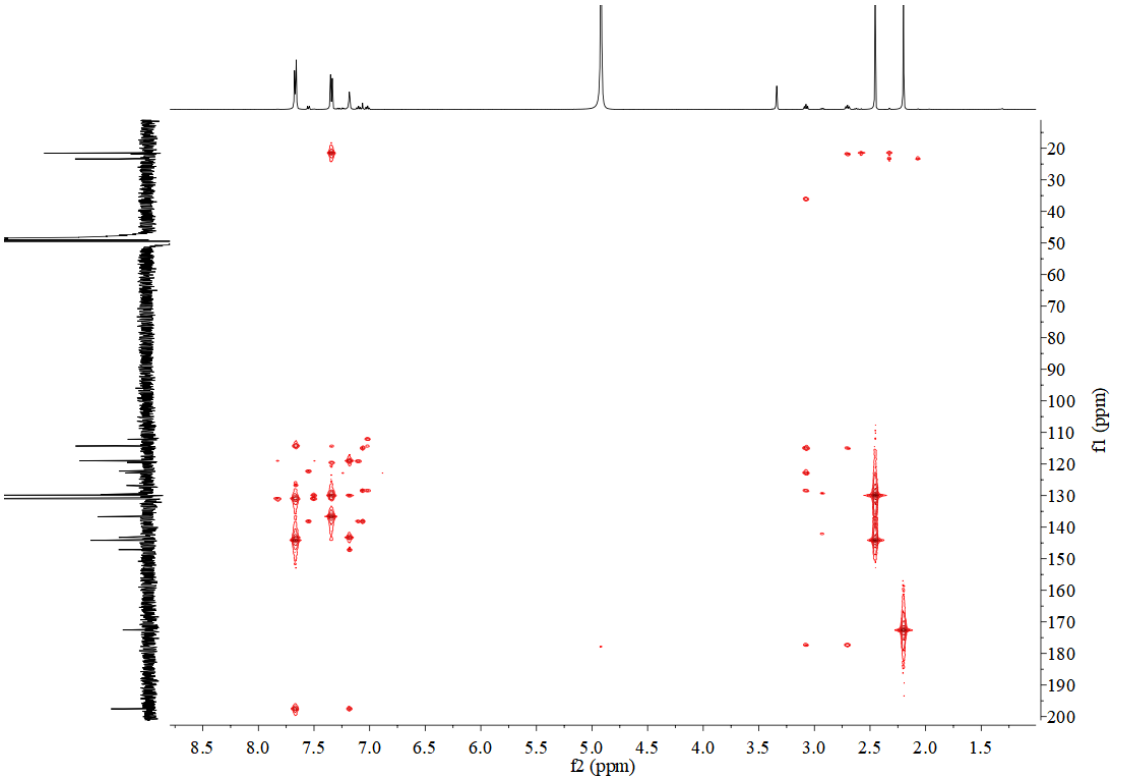

Figure 12. HMBC spectrum (500 MHz) of purified *N*-acetylamino-tolcapone in MeOD.

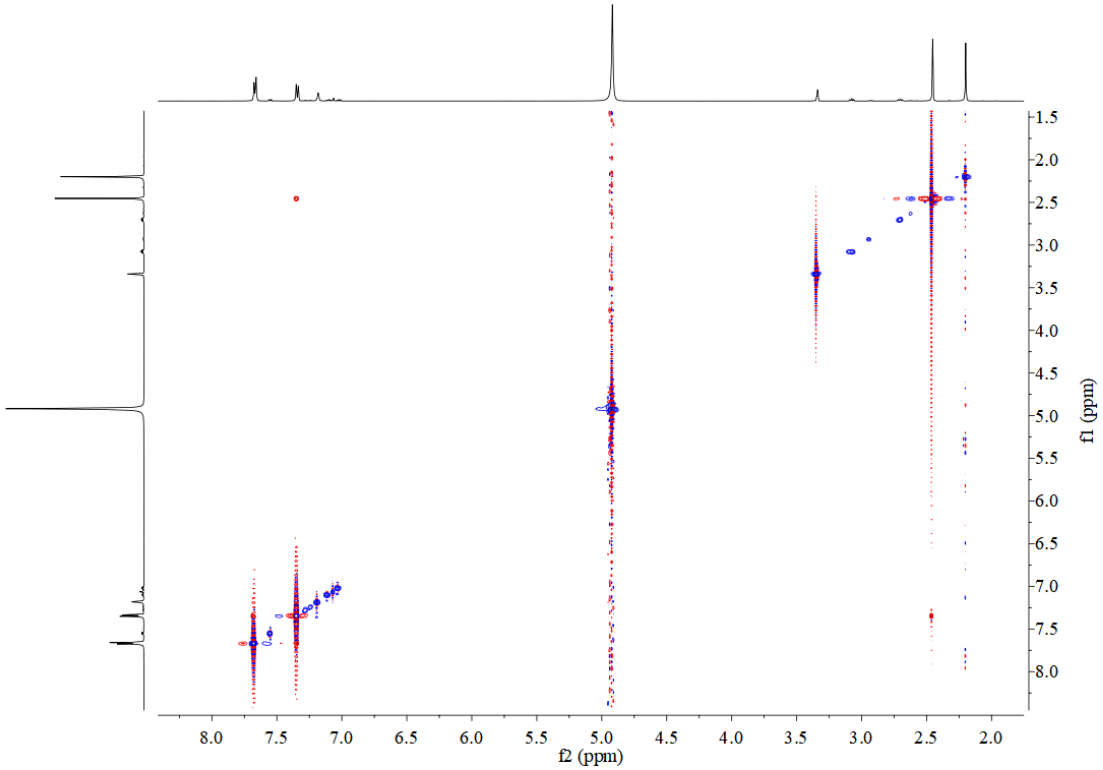

Figure 13. NOESY spectrum (500 MHz) of purified *N*-acetylamino-tolcapone in MeOD.

D. Misoprostol and misoprostol acid

The misoprostol metabolite was purified and its structure was elucidated using 1D and 2D NMR analyses.

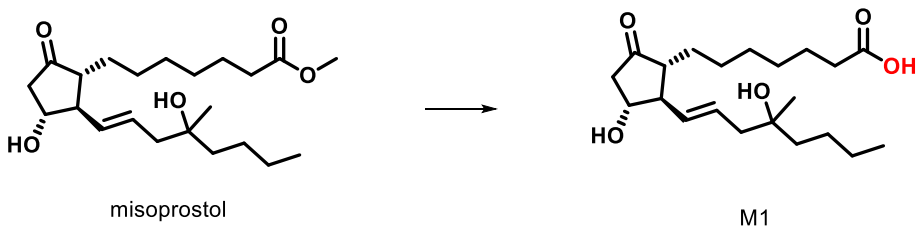

Figure 14. Misoprostol metabolism into misoprostol acid.

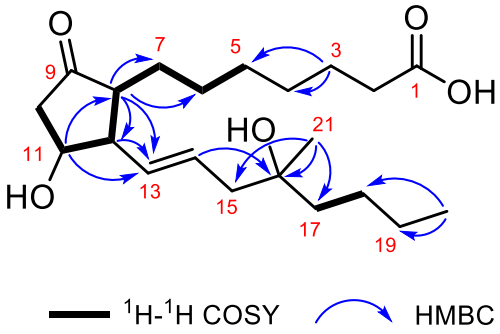

Figure 15. ^{1}H-^{1}H COSY, key HMBC correlations of purified misoprostol acid.

Table 4. ^{1}H and ^{13}C NMR data (δ in ppm, J in Hz) for purified misoprostol acid in MeOD.

No.	**M1**[a]	
	δ_H (mult)	δ_C type
1	–	168.8 qC
2	1.45 m	42.0 CH_2
3	1.58[b] m	26.2 CH_2
4	1.33[b] m	30.1 CH_2
5	1.33[b] m	30.6 CH_2
6	1.58[b] m	28.6 CH_2
7	1.33[b] m	27.7 CH_2
8	2.07 m	55.7 CH
9	–	217.9 qC
10	2.11 m, 2.68 m	47.4 CH_2
11	4.05 td (9.0, 7.5)	72.9 CH
12	2.35 m	55.5 CH
13	5.47 m	134.5 CH
14	5.68 m	130.5 CH
15	2.24 m	46.0 CH_2
16	–	73.3 qC
17	1.47 m	42.6 CH_2
18	1.37 m	27.0 CH_2
19	1.35 m	24.5 CH_2
20	0.93 t (7.0)	14.5 CH_3
21	1.15 s	26.7 CH_3

[a] Recorded at 500 MHz and 125 MHz for ^{1}H and ^{13}C NMR, respectively, in MeOD, chemical shifts (ppm) referred to MeOH (δ_H 3.31, δ_C 49.0). [b] overlapped. Assignments were deduced by analysis of 1D and 2D NMR spectra.

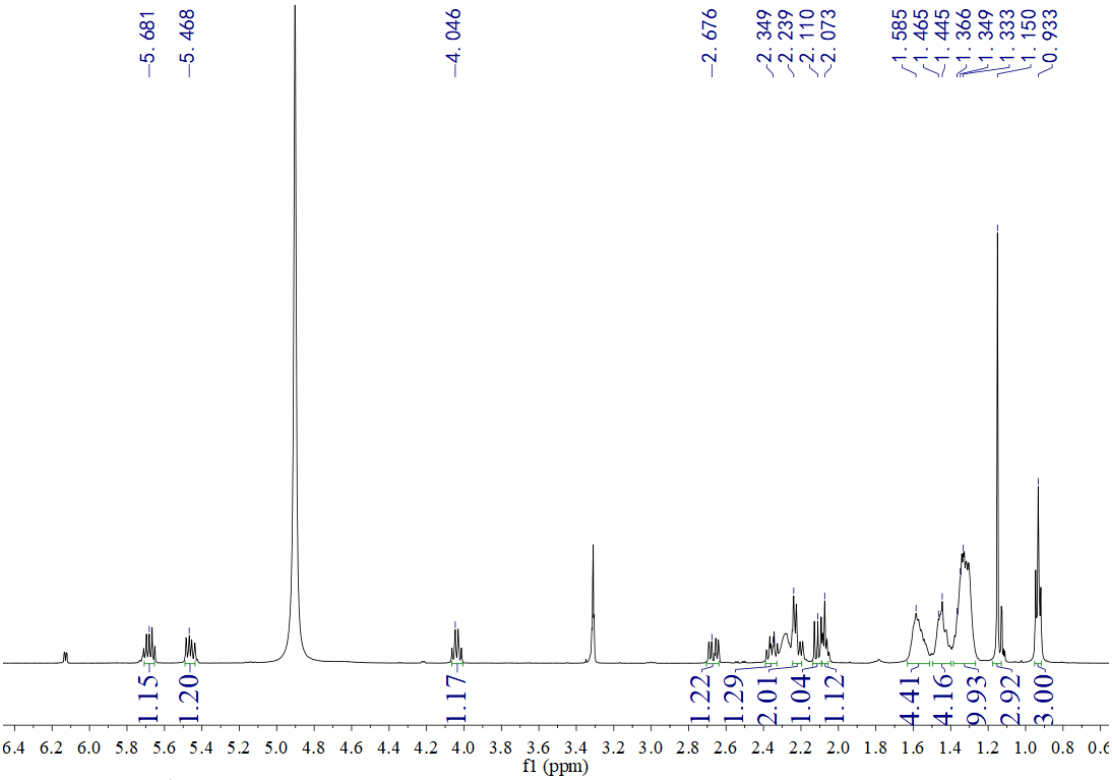

Figure 16. ^{1}H NMR spectrum (500 MHz) of purified misoprostol acid in MeOD.

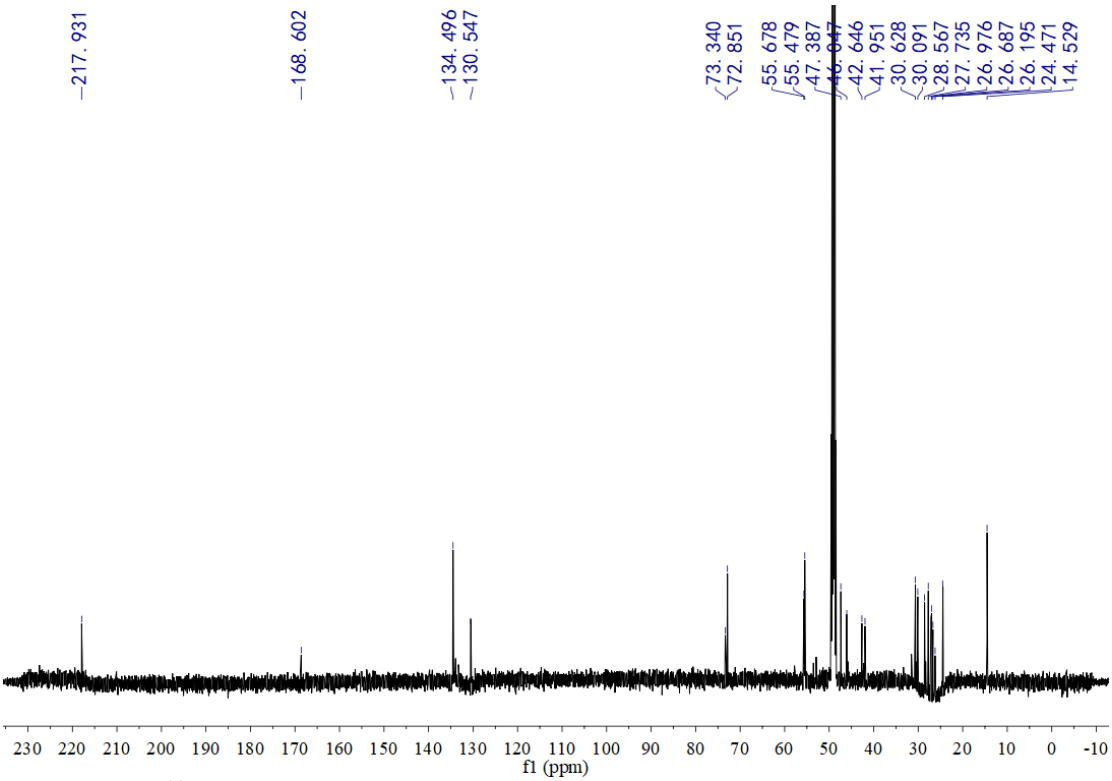

Figure 17. ^{13}C NMR spectrum (125 MHz) of purified misoprostol acid in MeOD.

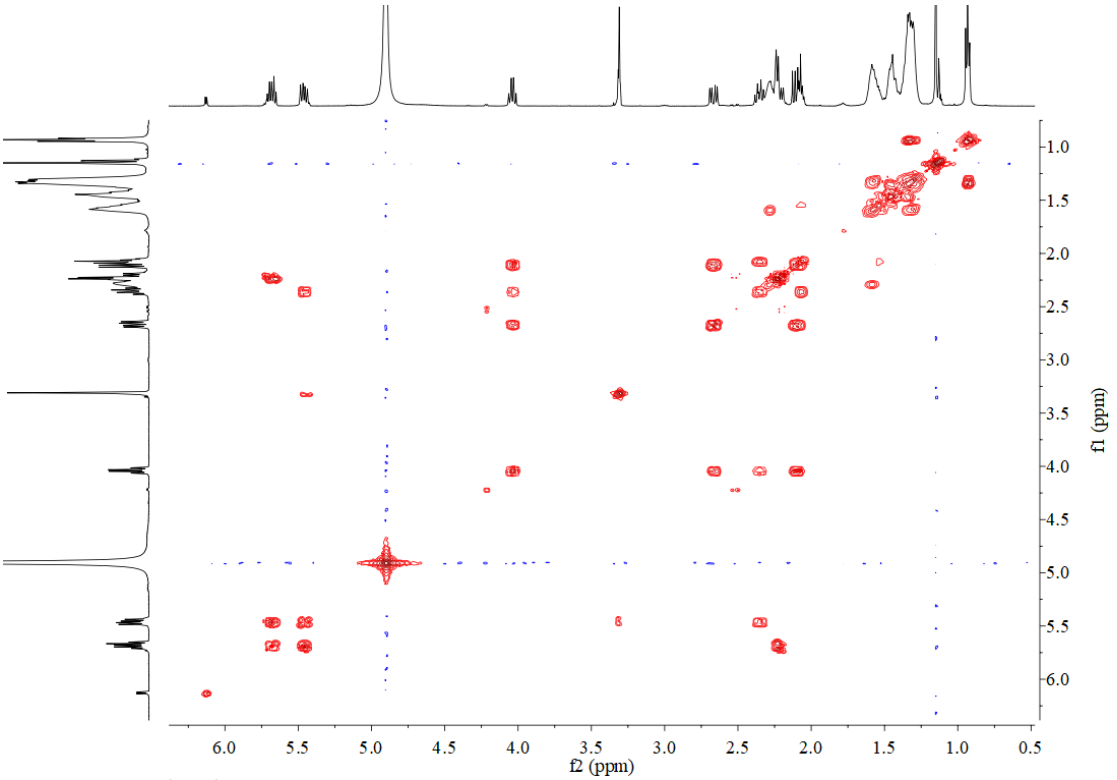

Figure 18. ^{1}H-^{1}H COSY spectrum (500 MHz) of purified misoprostol acid in MeOD.

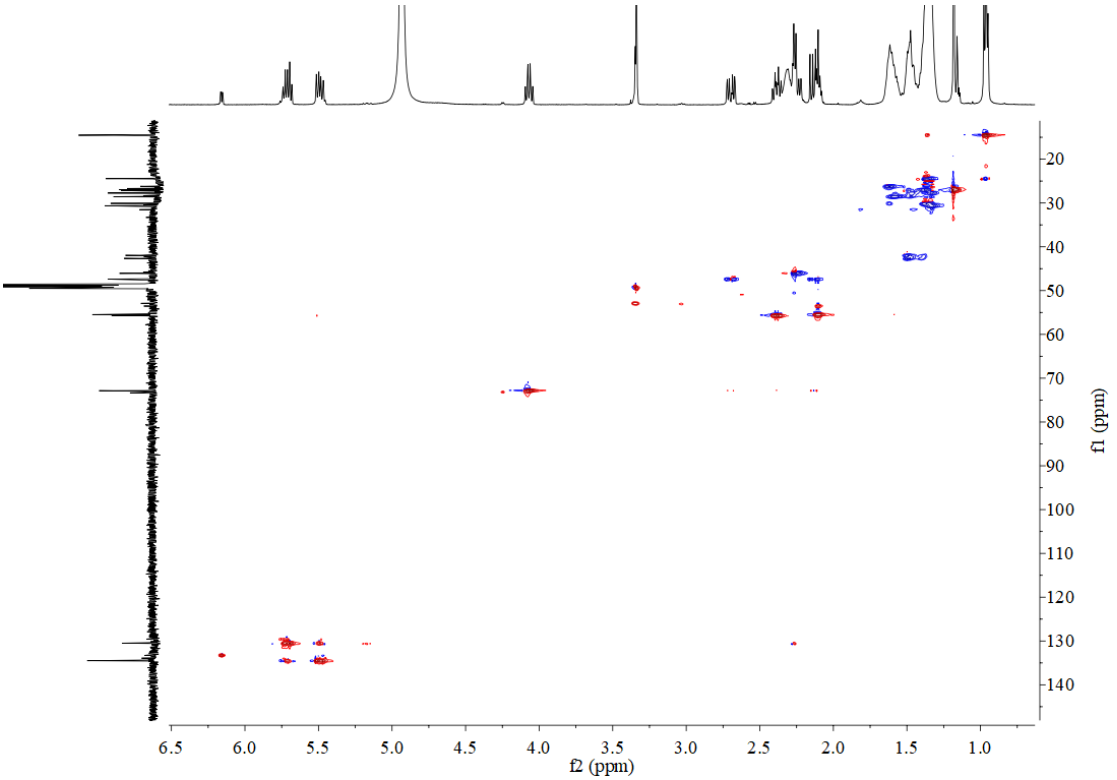

Figure 19. HSQC spectrum (500 MHz) of purified misoprostol acid in MeOD.

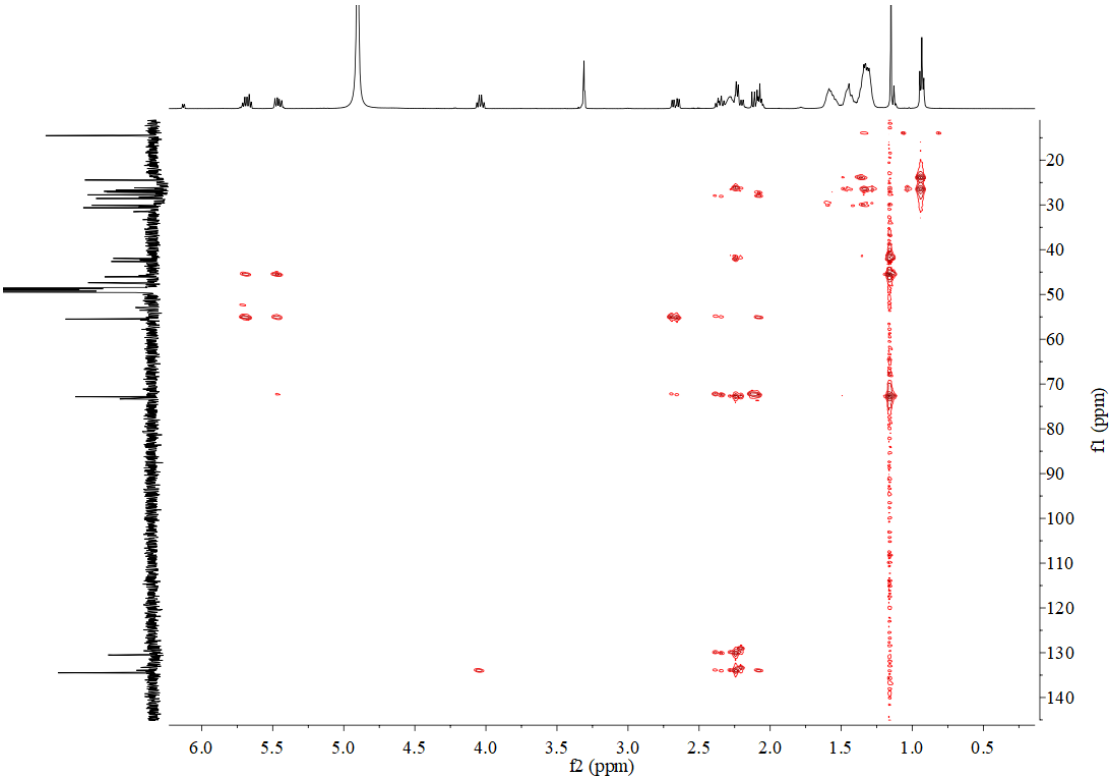

Figure 20. HMBC spectrum (500 MHz) of purified misoprostol acid in MeOD.

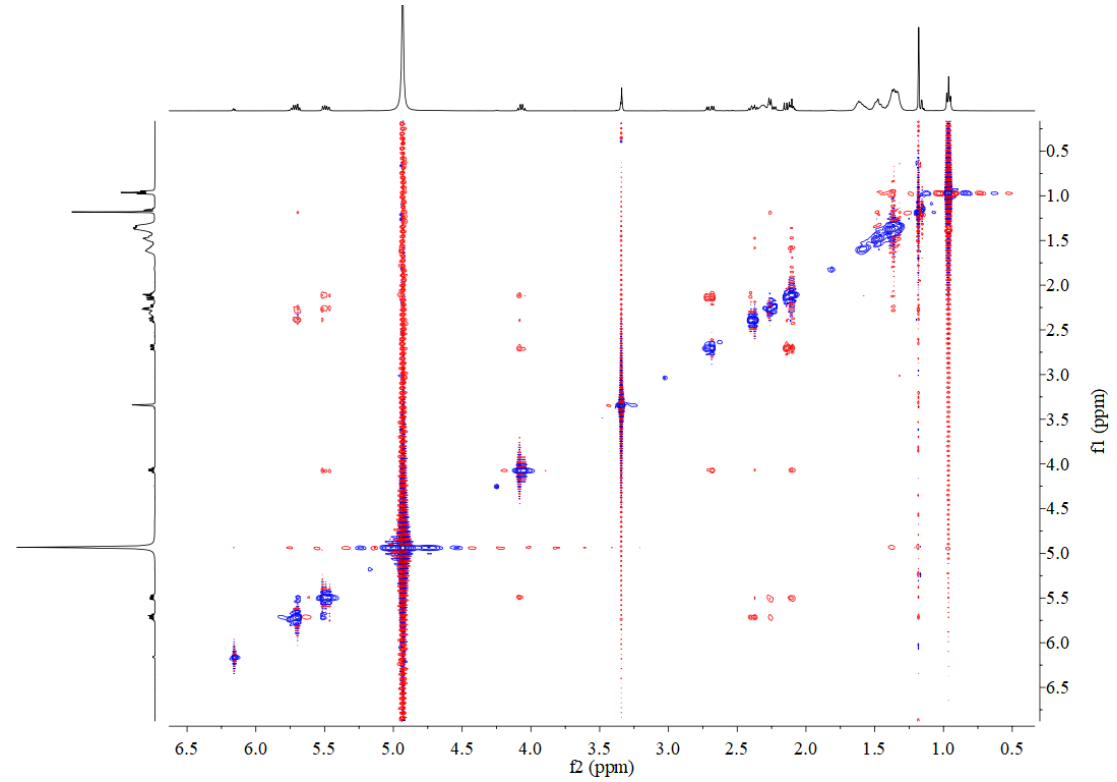

Figure 21. NOESY spectrum (500 MHz) of purified misoprostol acid in MeOD.

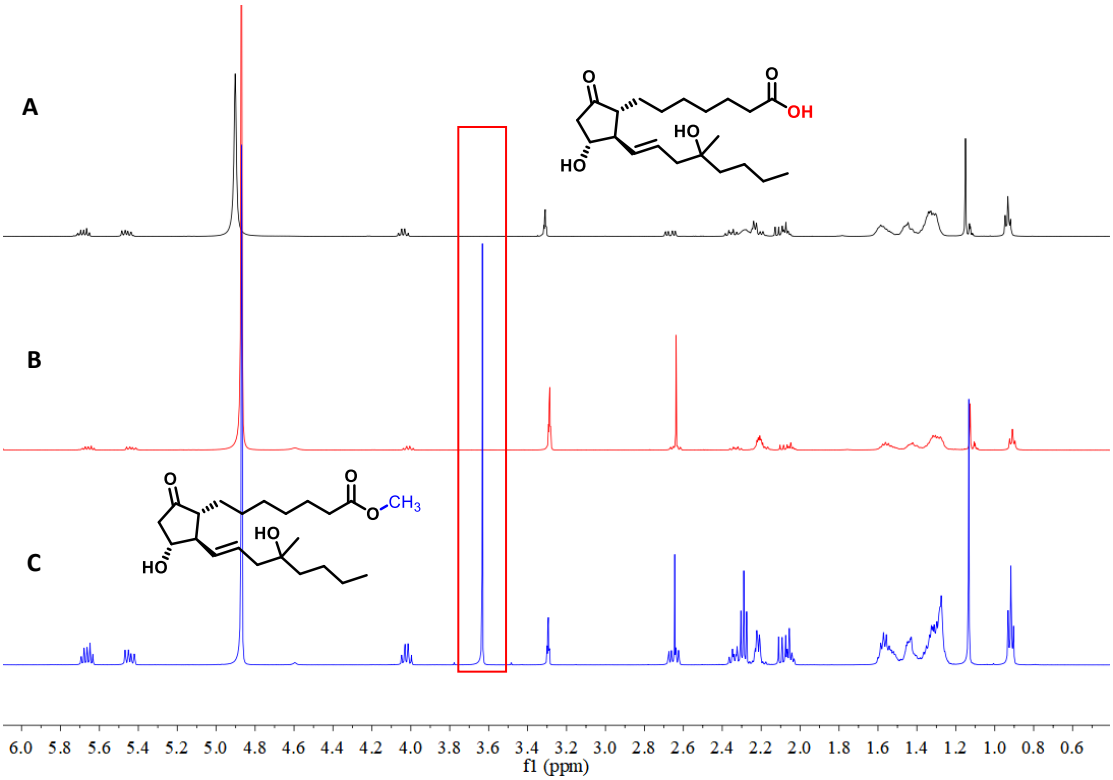

Figure 22. ^{1}H NMR spectrum (500 MHz) comparison between purified misoprostol acid (A), misoprostol free acid authentic standard (B), and misoprostol (C) in MeOD.

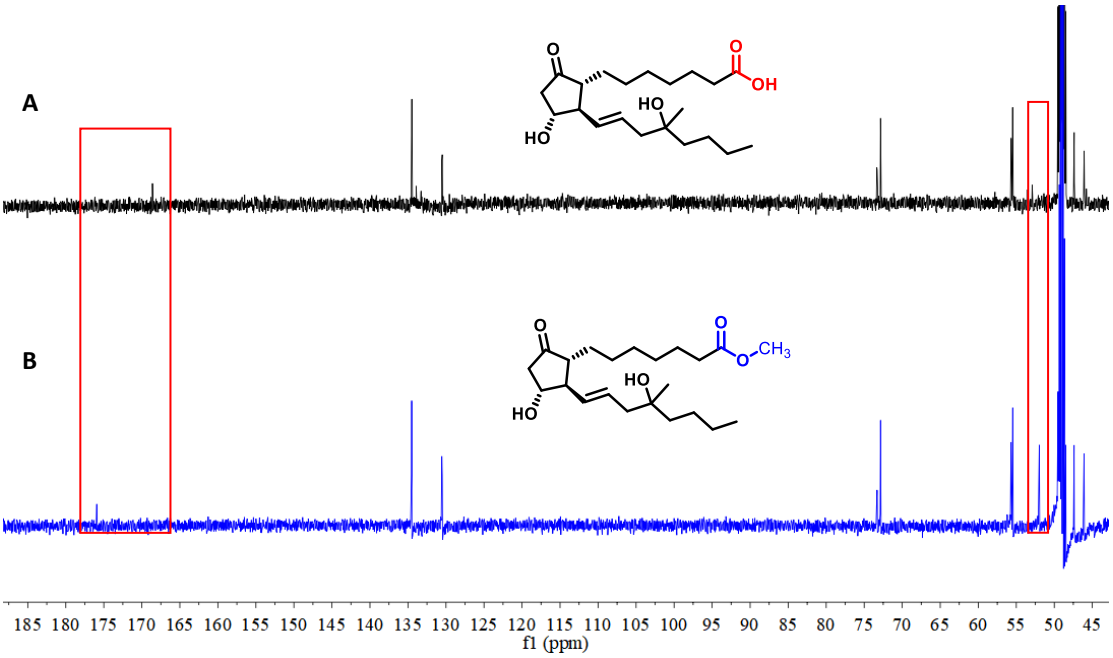

Figure 23. ^{13}C NMR spectrum (125 MHz) comparison between purified misoprostol acid (A) and misoprostol (B) in MeOD.

E. Mycophenolate mofetil and mycophenolic acid

The mycophenolate mofetil metabolite was determined to be mycophenolic acid by comparison to an authentic standard of mycophenolic acid using HPLC-HRMS/MS analysis following the same column, gradient, and analysis methods as for the donor runs (**Figures 24-26**). Isolated mycophenolic acid from *ex vivo* incubations of the PD microbiome with mycophenolate mofetil has the same retention time, accurate mass, and HRMS/MS fragmentation pattern as the authentic standard of mycophenolic acid.

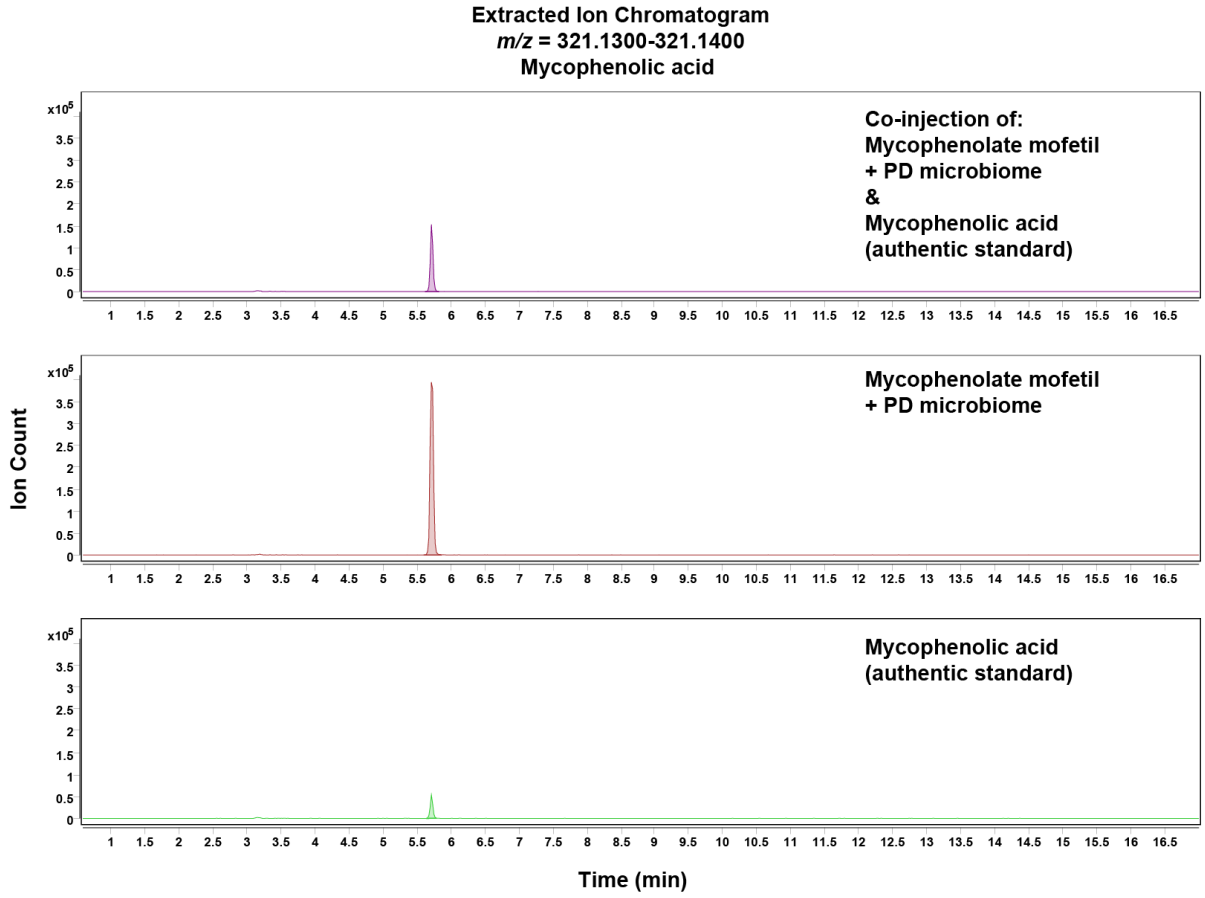

Figure 24. HPLC-HRMS analysis (Extracted Ion Chromatogram) of mycophenolic acid isolated from *ex vivo* incubations of the PD microbiome with mycophenolate mofetil, an authentic standard of mycophenolic acid, and a co-injection of both samples.

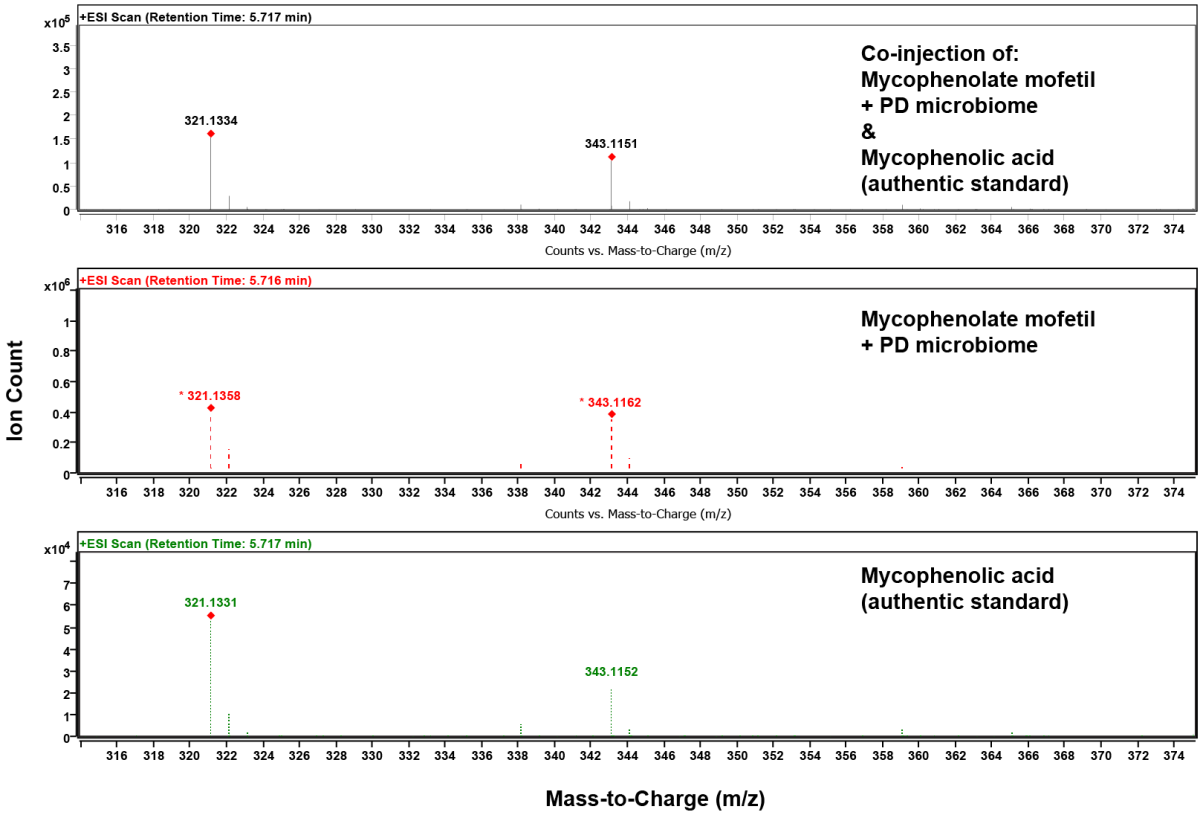

Figure 25. HPLC-HRMS analysis (Mass Spectrum) of mycophenolic acid isolated from *ex vivo* incubations of the PD microbiome with mycophenolate mofetil, an authentic standard of mycophenolic acid, and a co-injection of both samples.

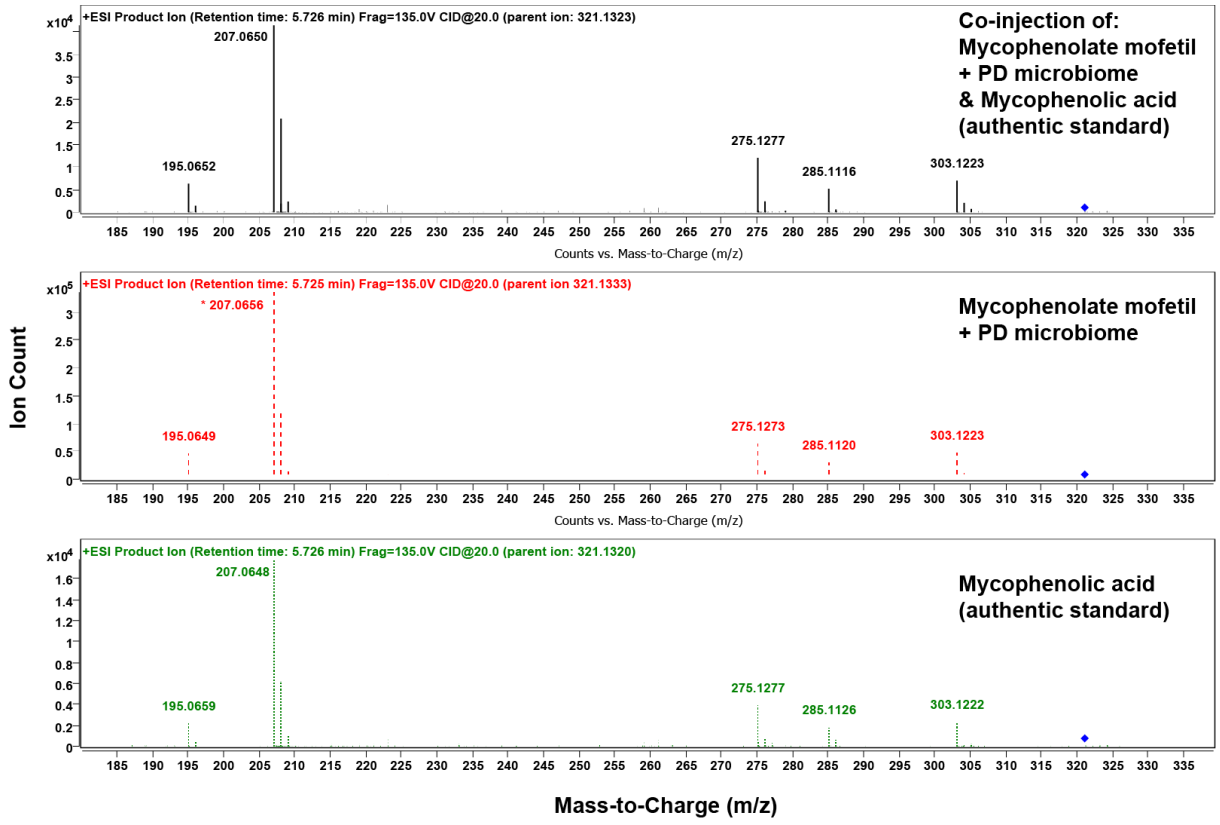

Figure 26. HPLC-HRMS/MS analysis (MS/MS Spectrum) of mycophenolic acid isolated from *ex vivo* incubations of the PD microbiome with mycophenolate mofetil, an authentic standard of mycophenolic acid, and a co-injection of both samples.

F. Spironolactone and 7α-thiospironolactone

The spironolactone metabolite was determined to be 7α-thiospironolactone by comparison to an authentic standard of 7α-thiospironolactone using HPLC-HRMS/MS analysis following the same column, gradient, and analysis methods as for the donor runs (**Figures 27-29**). Isolated 7α-thiospironolactone from *ex vivo* incubations of the PD microbiome with spironolactone has the same retention time, accurate mass, and HRMS/MS fragmentation pattern as the authentic standard of 7α-thiospironolactone.

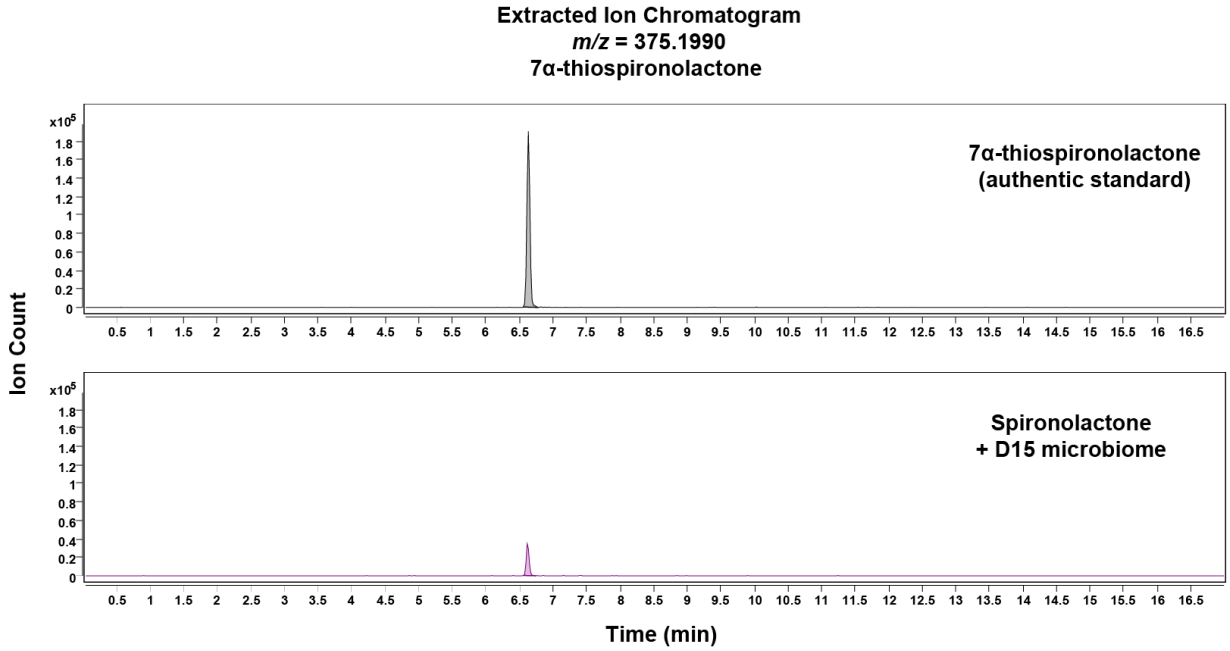

Figure 27. HPLC-HRMS analysis (Extracted Ion Chromatogram) of 7α-thiospironolactone isolated from *ex vivo* incubations of the D15 microbiome with spironolactone and an authentic standard of 7α-thiospironolactone, showing that they elute at the same retention time.

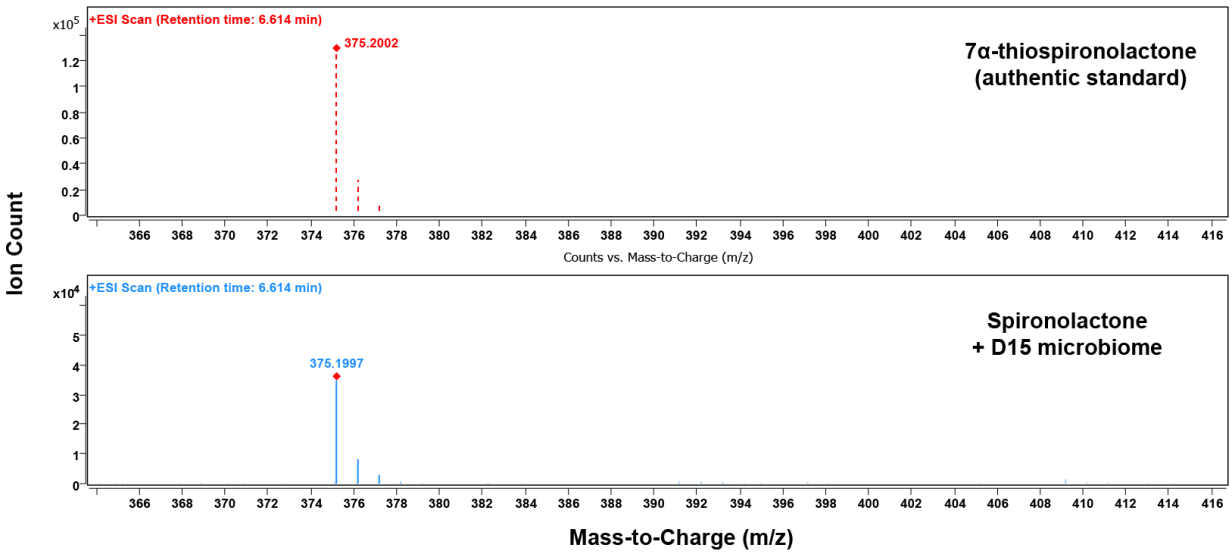

Figure 28. HPLC-HRMS analysis (MS spectrum) of 7α-thiospironolactone isolated from *ex vivo* incubations of the D15 microbiome with spironolactone and an authentic standard of 7α-thiospironolactone.

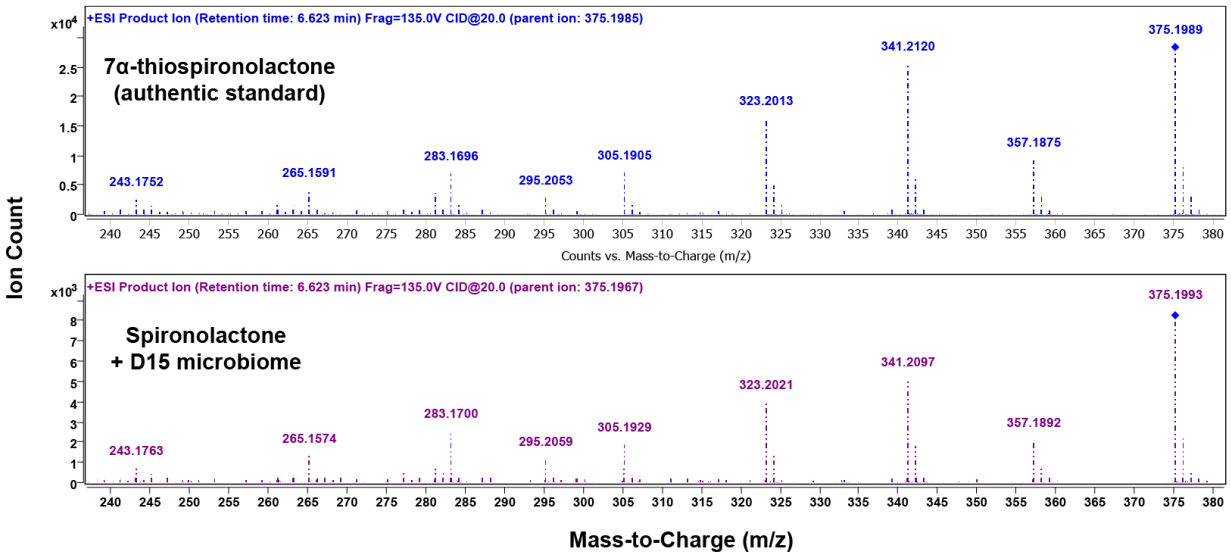

Figure 29. HPLC-HRMS analysis (MS/MS spectrum) of 7α-thiospironolactone isolated from *ex vivo* incubations of the D15 microbiome with spironolactone and an authentic standard of 7α-thiospironolactone.